

Quantum Annealing Based Difficulty Adjustable Maze Generation

Yuto Ishikawa^{1,*}, Takuma Yoshihara^{2,*}, Keita Okamura^{3,*} and Masayuki Ohzeki^{4,5,6}

¹Department of Computer Science, Nagoya University, Nagoya, Aichi, Japan

²Department of Engineering, Tokyo Denki University, Adachi, Tokyo, Japan

³Department of Science and Technology, Tokyo University of Science, Noda, Chiba, Japan

⁴Graduate School of Information Sciences, Tohoku University Sendai, Miyagi, Japan

⁵Department of Physics, Tokyo Institute of Technology, Meguro, Tokyo, Japan

⁶Sigma-i Co., Ltd., Shinagawa, Tokyo, Japan

Correspondence*:

Corresponding Author

ishikawa.yuto.f6@s.mail.nagoya-u.ac.jp

21ef106@ms.dendai.ac.jp

6223024@ed.tus.ac.jp

ABSTRACT

In this paper, the maze generation using quantum annealing is proposed. We reformulate a standard algorithm to generate a maze into a specific form of a quadratic unconstrained binary optimization problem suitable for the input of the quantum annealer. To generate more difficult mazes, we introduce an additional cost function Q_{update} to increase the difficulty. The difficulty is evaluated by the time to solve the maze. To check the efficiency of our scheme to create the maze, we investigated the time-to-solution of a quantum processing unit, classical computer, and hybrid solver.

Keywords: quantum annealing, combinatorial optimization, maze generation, bar-tipping algorithm, time-to-solution

1 INTRODUCTION

A combinatorial optimization problem is minimizing or maximizing their cost or objective function among many variables that take discrete values. In general, it takes time to solve the combinatorial optimization problem. To deal with many combinatorial optimization problems, we utilize generic solvers to solve them efficiently. Quantum annealing (QA) is one of the generic solvers for solving combinatorial optimization problems Kadowaki and Nishimori (1998) using the quantum tunneling effect. Various applications of QA are proposed in traffic flow optimization Neukart et al. (2017); Hussain et al. (2020); Inoue et al. (2021), finance Rosenberg et al. (2016); Orús et al. (2019); Venturelli and Kondratyev (2019), logistics Feld et al. (2019); Ding et al. (2021), manufacturing Venturelli et al. (2016); Yonaga et al. (2022); Haba et al. (2022), preprocessing in material experiments Tanaka et al. (2023), marketing Nishimura et al. (2019), steel manufacturing Yonaga et al. (2022), and decoding problems Ide et al. (2020); Arai et al. (2021a). The model-based Bayesian optimization is also proposed in the literature

Koshikawa et al. (2021) A comparative study of quantum annealer was performed for benchmark tests to solve optimization problems Oshiyama and Ohzeki (2022). The quantum effect on the case with multiple optimal solutions has also been discussed Yamamoto et al. (2020); Maruyama et al. (2021). As the environmental effect cannot be avoided, the quantum annealer is sometimes regarded as a simulator for quantum many-body dynamics Bando et al. (2020); Bando and Nishimori (2021); King et al. (2022). Furthermore, applications of quantum annealing as an optimization algorithm in machine learning have also been reported Neven et al. (2012); Khoshaman et al. (2018); O'Malley et al. (2018); Amin et al. (2018); Kumar et al. (2018); Arai et al. (2021b); Sato et al. (2021); Urushibata et al. (2022); Hasegawa et al. (2023); Goto and Ohzeki (2023). In this sense, developing the power of quantum annealing by considering hybrid use with various techniques is important, as in several previous studies Hirama and Ohzeki (2023); Takabayashi and Ohzeki (2023).

In this study, we propose the generation of the maze by quantum annealing. Several algorithms for the generation of the maze have been proposed. One can take the bar-tipping algorithm Alg (2023a), the wall-extending algorithm Alg (2023b), and the hunt-and-kill algorithm Alg (2023c).

In the bar-tipping algorithm, an inner wall is placed every two cells inside an outer wall, and the inner wall is used as a bar, which is then knocked down one by one in turn. It requires the following three constraints. First, each bar can only be knocked down in one direction. Second, the first column can be knocked down in four directions: up, down, left, and right, while the second and subsequent columns can be knocked down only in three directions: up, down, and right. These two constraints are to prevent closed paths by eliminating them. Third, adjacent bars cannot be knocked in the same direction. This is to prevent multiple maze solutions. If multiple solutions are possible, the maze solution is not unique, simplifying the time and difficulty of reaching the maze goal. The bar-tipping algorithm can generate the maze by satisfying the above three constraints.

The wall-extending algorithm is an algorithm that generates a maze by extending and creating walls from a situation where the entire surface is a path. First, as an initial condition, the outer perimeter of the maze is assumed to be the outer wall, and the rest of the maze is assumed to be the pathway. The coordinates where both x and y are even are listed as the starting coordinates for wall extending. The coordinates are taken randomly from the wall extension start coordinates, which are not walls, and the following process is carried out. Randomly determine the next direction of extending with the specified coordinate as a wall. The extension will be repeated until the direction to be extended is a path. These processes are repeated until all the coordinates change to the walls.

The entire surface is initially walled off in the hunt-and-kill algorithm. A point is chosen randomly, and the path is extended from there. If the path can no longer be extended, a point is randomly selected from an already created and extended path. This process is repeated to generate the maze.

Of the three maze generation algorithms mentioned above, the bar-tipping algorithm is relevant to the combinatorial optimization problem. Thus, we have chosen to deal with this algorithm. Using the bar-tipping algorithm, we reformulated it to solve a combinatorial optimization problem that generates a maze with a longer solving time and optimized it using quantum annealing. Quantum annealing, classical computing, and hybrid computing were compared with each other according to the generation time of mazes, and their performance was evaluated. We do not use an exact solver to solve the combinatorial optimization problem. We expect some diversity in the solution and not only focus on the optimal solution in maze generation. Thus, we compare three solvers, which generate various solutions.

The paper is organized as follows. In the next Section, we explain the methods of our experiments. In Sec. 3, we describe the results of our experiments. In Sec. 4, we summarize this paper.

2 METHODS

2.1 Cost function

To generate the maze by quantum annealer, we need to set the cost function in the quantum annealer. One of the important features of the generation of the maze is diversity. In this sense, the optimal solution is not always unique. Since it is sufficient to obtain a structure consistent with a maze, the cost function is mainly derived from the necessary constraints of a maze, as explained below. Three constraints describe the basis of the algorithm of the bar-tipping algorithm. The available cost function in the quantum annealer is only the quadratic function. The cost function will be converted to a QUBO matrix to use the quantum annealer. Here, QUBO implies quadratic unconstrained binary optimization. Using the penalty method, we can convert various constraints written in a linear form into a quadratic function. Thus, we construct the cost function for generating the maze using the bar-tipping algorithm below.

The first constraint of the bar-tipping algorithm is that the bars can be knocked down in only one direction. It prevents making closed circuits. The second constraint of the bar-tipping algorithm is that the bars of the first column be knocked down randomly in four directions (up, right, down, and left), and the second and subsequent columns can be knocked down randomly in three directions (up, right, and down). It also prevents the creation of closed circuits. The third constraint of the bar-tipping algorithm is that adjacent bars must not overlap. Following the constraint in the bar-tipping algorithm, we can generate a maze with only one path from the start to the goal.

In this study, a maze generated by knocking down the $N \times N$ bars is called $N \times N$ maze.

The cost function consists of three terms to reproduce the bar-tipping algorithm according to the three constraints and to determine the start and goal.

$$E(\{x_{i,j,d}, X_{m,n}\}) = \sum_{i,i'} \sum_{j,j'} \sum_{d,d'} Q_{(i,j,d),(i',j',d')} x_{i,j,d} x_{i',j',d'} + \lambda_1 \sum_i \sum_j \left(\sum_d x_{i,j,d} - 1 \right)^2 + \lambda_2 \left(\sum_m \sum_n X_{m,n} - 2 \right)^2, \quad (1)$$

where $x_{i,j,d}$ denotes whether the bar in i -th row, j -th column knocked down in direction d (up: 0, right: 1, down: 2, left: 3). Due to the second constraint of the bar-tipping algorithm, the bars after the second column cannot be knocked down on the left side; only the first column has ($d = 3$). Furthermore, $Q_{(i,j,d),(i',j',d')}$ in Equation 1 depends on i, j, d, i', j' , and d' and is expressed as follows

$$Q_{(i,j,d),(i',j',d')} = \begin{cases} 1 & (i = i' - 1, j = j', d = 2, d' = 0) \\ 1 & (i = i' + 1, j = j', d = 0, d' = 2) \\ 0 & \text{otherwise.} \end{cases} \quad (2)$$

The first term prevents the bars from overlapping and falling over each other. It represents the third constraint of the bar-tipping algorithm. $Q_{(i,j,d),(i',j',d')}$ is QUBO matrix. If the bars in $(i, j), (i', j')$ overlap in adjacent rows of the same column, it takes the value 1. Otherwise, it takes the value 0. Due to the second

constraint, bars in the second and subsequent columns cannot be knocked down to the left. Adjacent bars in the same row thus cannot overlap. The second term is a penalty term that limits the direction of tipping to one per bar. It represents the first constraint of the bar-tipping algorithm. This means that for a given coordinate (i, j) , the sum of $x_{(i,j,d)}$ must take the value 1. In the third term, we use $X_{m,n}$, which denotes whether or not to set the start and goal at the m -th row and n -th column of options of start and goal coordinates. There are no relation between $X_{m,n}$ and $x_{i,j,d}$ in Equation 1. This means there is no relation between the maze structure, the coordinates of the start, and goal determination. Here, (m, n) is different from the coordinate setting bars; it is located at the four corners of the bars, where the bars do not tip. Figure 1 shows where coordinates (m, n) are. The third term is the penalty term for selecting

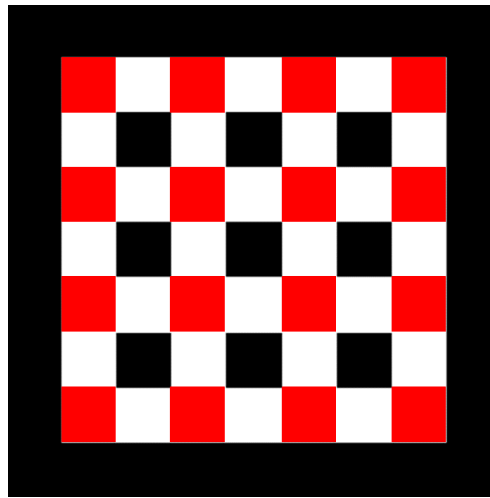


Figure 1. Black cells represent outer walls and inner bars (i, j) . Red cells represent options of start and goal coordinates (m, n) .

two coordinates of the start and the goal from the coordinates (m, n) . The start and goal are randomly selected from the two coordinates determined by the third term. This is because the start and the goal are commutative in the maze.

We have shown the simplest implementation of the maze generation following the bar-tipping algorithm by quantum annealer. We add the effect to make the maze more difficult in the cost function.

2.2 Update rule

We propose an additional Q_{update} term to increase the time to solve the maze. We introduce a random term that takes random elements to change the maze structure. First, Q_{update} term, the additional term

which includes the new QUBO matrix Q_{update} , is given by

$$\begin{aligned}
 & \lambda_{update1} \sum_{i,i'} \sum_{j,j'} \sum_{d,d'} Q_{update(k,k')} x_{i,j,d} x_{i',j',d'} \\
 & + \lambda_{update1} \sum_i \sum_j \sum_d \sum_m \sum_n Q_{update(k,l)} x_{i,j,d} X_{m,n} \\
 & + \lambda_{update1} \sum_i \sum_j \sum_d \sum_m \sum_n Q_{update(l,k)} X_{m,n} x_{i,j,d} \\
 & + \lambda_{update2} \sum_{m,m'} \sum_{n,n'} Q_{update(l,l')} X_{m,n} X_{m',n'},
 \end{aligned} \tag{3}$$

where

$$\begin{cases} k = d + 4j + (3N + 1)i & (i = 0) \\ k = d + 3j + 1 + (3N + 1)i & (i \neq 0) \\ l = (3N + 1)N + (N + 1)m + n. \end{cases} \tag{4}$$

Here, k', l' are the replacement of i, j, m, n in k, l with i', j', m', n' . The coefficients $\lambda_{update1}$ and $\lambda_{update2}$ were defined to multiply the elements of the Q_{update} for maze generating and the elements of the Q_{update} for start and goal determination, respectively. When these values are the same, a maze is generated in which the constraints are violated. These are to control the maze difficulty without breaking the bar-tipping algorithm's constraints. Equation 3 is represented by the serial number k of each coordinate (i, j) at which bars can tip, and the sum l of the total number of coordinates at which the bars can tip and the serial number of coordinates (m, n) , which are options for the start and the goal. In addition, Equation 3 allows the maze to consider the relation between the structure of the maze and the coordinates of the start and the goal.

Second, Q_{update} , the new QUBO matrix, is given by

$$Q_{update} := p(t)Q_{update} + \{1 - p(t)\}Q_{random}, \tag{5}$$

where Q_{random} is a matrix of random elements from -1 to 1 and $p(t)$ depends on time t taken to solve the previous maze and is expressed as follows

$$p(t) = \frac{1}{1 + e^{-at}}. \tag{6}$$

The longer the solving time t of the maze is, the higher the percentage of the previous Q_{update} in the current Q_{update} and the lower the percentage of Q_{random} ; inversely, when t is small, the ratio of the previous Q_{update} is small, and the percentage of Q_{random} is significant. In other words, the longer the solving time of the previous maze, the more characteristics of the previous term Q_{update} remain. Here, a is a constant to adjust the percentage.

2.3 Experiments

2.3.1 Generation of maze

We generate mazes by using DW_2000Q_6. The start, goal determination, and update terms were excluded for this experiment. $\lambda_1 = 2$ was chosen.

2.3.2 Computational cost

We compare the generation times of $N \times N$ maze in DW_2000Q_6, SASampler, SQASampler, hybrid_binary_quadratic_model_version2 (hereinafter referred to as "Hybrid Solver") and classical computer based on bar-tipping algorithm (hereinafter referred to as "Classic"). The start, goal determination, and update terms were excluded for this experiment. We set $\lambda_1 = 2$. Generation times for DW_2000Q_6 was calculated using time-to-solution (TTS). Regression curves were drawn from the results to examine the dependence of computation time on maze size.

2.3.3 Effect of update term

The solving time of 9×9 maze generated without Q_{update} and using Q_{update} were measured 30 times. Three players were asked to generate and solve a maze in this experiment. The players can only see the limited 5×5 cells. In other words, only two surrounding cells can be seen.

To investigate whether the update term affects mazes, figures of 30 mazes solved by players were overlaid.

3 RESULTS

3.1 Generation of maze

We generate mazes by using DW_2000Q_6 (Figure 2).

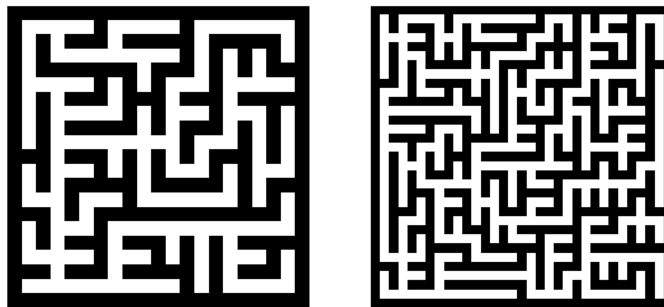


Figure 2. Left: 9×9 maze generated by DW_2000Q_6. Right: 15×15 maze generated by DW_2000Q_6.

3.2 Computational cost

DW_2000Q_6 seems to be $\mathcal{O}(7.41 \cdot 10^{-2} N^2)$ though its deviation is smaller than the others (Figure 3). Classic $\mathcal{O}(0.855 N^2)$, SASampler $\mathcal{O}(28.8 N^2)$, and SQASampler $\mathcal{O}(173 N^2)$ exhibit quadratic dependence on the maze size $\mathcal{O}(N^2)$ (Figure 4, 5, and 6). On the other hand, Hybrid Solver is $\mathcal{O}(1)$ or $\mathcal{O}(N)$ ($3.29 \cdot$

$10^{-4}N + 2.99$) between $N = 1$ and $N = 18$ and then shifted to $\mathcal{O}(N^2)$ ($7.00 \cdot 10^{-3}N^2 - 3.78 \cdot 10^{-4}N + 0.690$) (Figure 7).

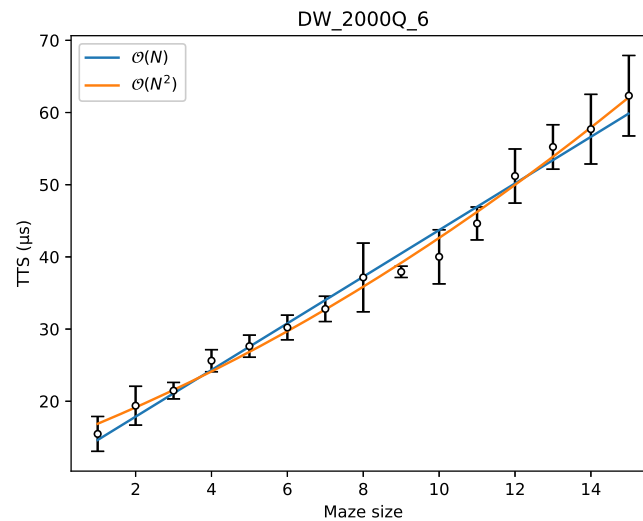


Figure 3. Time to reach the ground state with 99% success probability as a function of the maze size in DW_2000Q_6. The error bars represent a 95% confidence interval. The regression curve is given by $(7.41 \cdot 10^{-2}N^2 + 2.05N + 14.8)$.

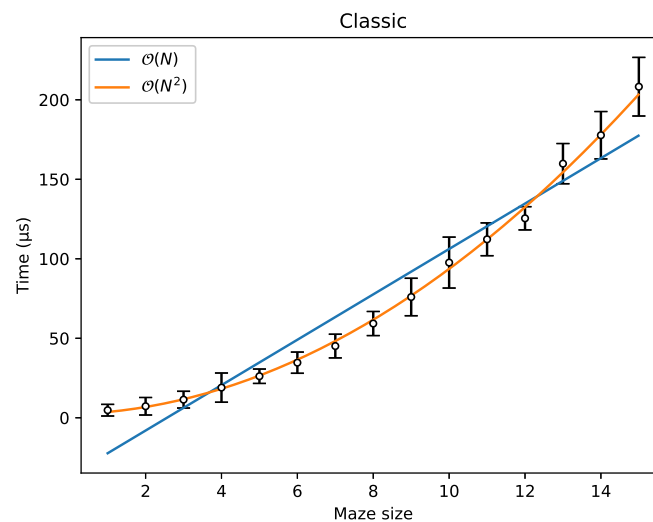


Figure 4. The time to reach the ground state as a function of the maze size in Classic. The error bars represent a 95% confidence interval. The regression curve is $(0.855N^2 + 0.601N + 2.16)$

3.3 Effect of update term

The simple moving average of ten solving times were plotted on the graph. For this experiment, $\lambda_1 = 2$, $\lambda_2 = 2$, $\lambda_{update1} = 0.15$, $\lambda_{update2} = 0.30$ and $a = 0.05$ were chosen.

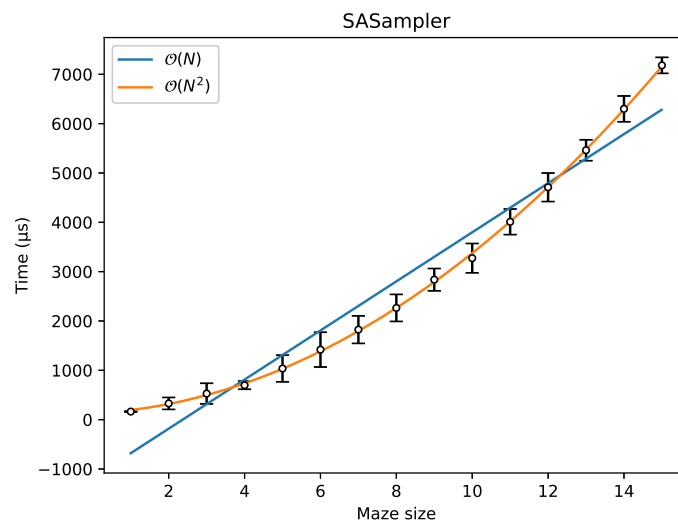


Figure 5. Time to reach the ground state as a function of the maze size in SASampler. The error bars represent a 95% confidence interval. The regression curve is $(28.8N^2 + 36.3N + 129)$

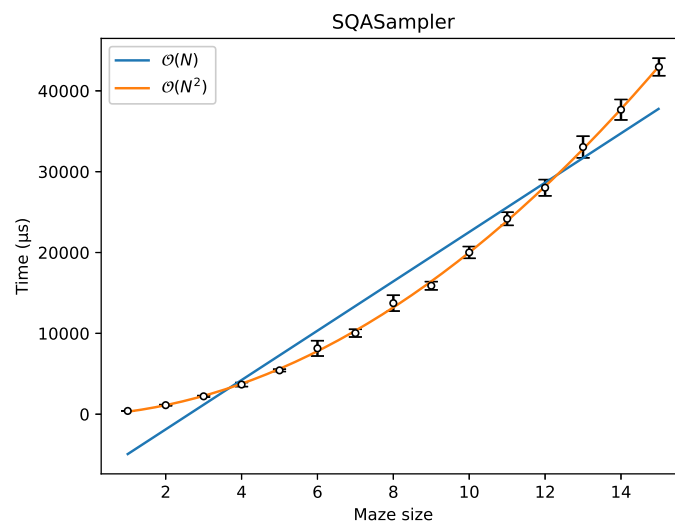


Figure 6. Time to reach the ground state as a function of the maze size in SQASampler. The error bars represent a 95% confidence interval. The regression curve is $(173N^2 + 287N - 150)$

As Figure 8 shows, the solving time of the maze without Q_{update} was getting shorter (PlayerA and PlayerB) or unstable, just like the mountain shape (PlayerC). The solving time of the maze using Q_{update} was getting longer (Figure 9). In addition, each player's average of the solving time of the maze generated using Q_{update} (PlayerA: 20.5s, PlayerB: 43.1s, PlayerC: 43.7s) increased than that of the maze generated without Q_{update} (PlayerA: 19.6s, PlayerB: 37.1s, PlayerC: 41.2s).

There are no patterns in the mazes generated without Q_{update} (Figure 10). Each player's maze generation patterns seem to differ (Figure 11). However, these patterns depend on random elements rather than players since the patterns are different, even if the same player solves the maze several times. (Figure 12).

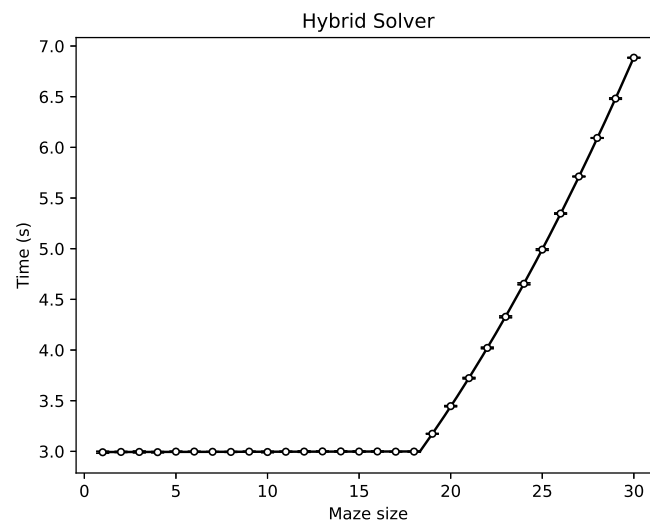


Figure 7. Time to reach the ground state as a function of maze size in the Hybrid Solver. The error bars represent a 95% confidence interval.

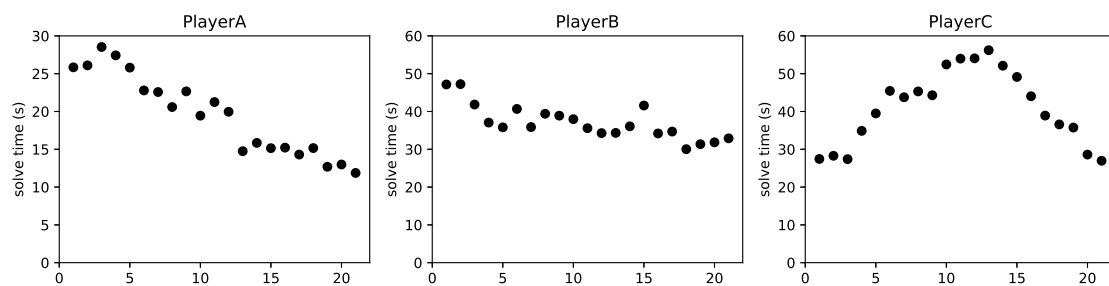


Figure 8. Average of 10 solving time of 9×9 maze generated without Q_{update} .

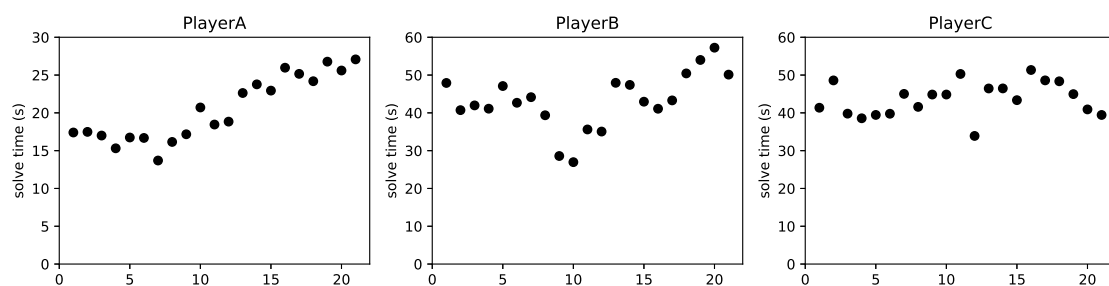


Figure 9. Average of 10 solving time of 9×9 maze generated using Q_{update} .

We should emphasize that although no particular pattern appears strongly and there does not seem to be any individual habit, there are differences in the time it takes to solve the mazes.

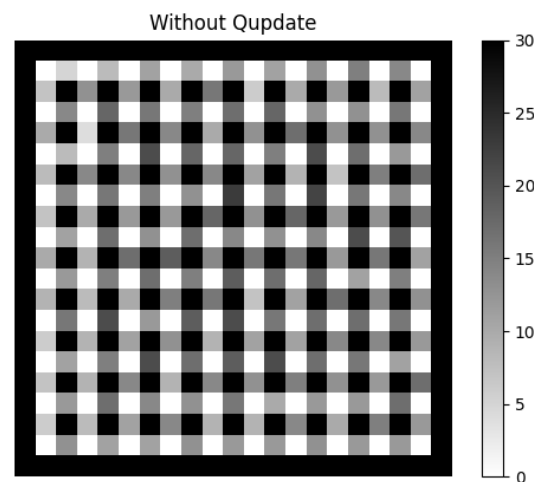


Figure 10. Overlaid 30 mazes generated without Q_{update} .

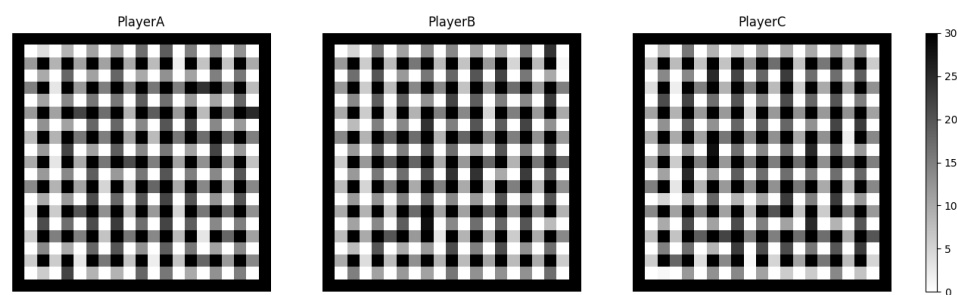


Figure 11. Each player's overlaid 30 mazes generated using Q_{update} .

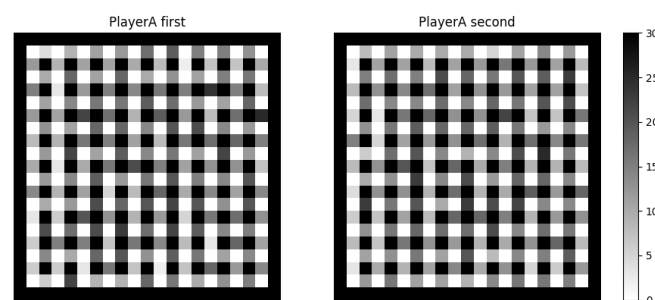


Figure 12. The same player's overlaid 30 mazes generated using Q_{update} .

4 DISCUSSION

In this paper, we demonstrated that the more difficult maze generation with the bar-tipping algorithm is still possible with quantum annealing. By reformulating the bar-tipping algorithm as the combinatorial

optimization problem, we generalize it more flexibly to generate mazes. In particular, our approach is simple but can adjust the difficulty in solving mazes by quantum annealing.

In this study, we proposed Q_{update} to increase the solving time using quantum annealing. We demonstrated that introducing Q_{update} increased the time to solve the maze and changed the difficulty compared to the case where Q_{update} was not introduced. At this time, we needed to adjust constants a , $\lambda_{update1}$, and $\lambda_{update2}$ in Equations 3 and 6 to change the maze difficulty.

In our investigation, Q_{update} can be applied to the problem of determining the difficulty of the next state from the previous result. The selection of personalized educational materials is one of the examples. Based on the solving time of the previously solved problems, the educational materials can be selected at a difficulty suitable for the individual. This is the most fascinating direction in future studies.

Other maze-generation algorithms would also be generalized by reformulation as combinatorial optimization problems. The wall-extending and hunt-and-kill algorithms will be implemented in future studies by considering the following ingredients. We should introduce a state with a rule that if an adjacent bar is knocked down, it will also be knocked down in the former algorithm. For the latter, we compute the number of connected components and then include its result in optimization. Similarly to our approach in this study, their reformulations make it difficult to solve mazes according to the original algorithms.

Regarding comparing computational costs to solve our approach to generating mazes using TTS, DW_2000Q_6 has a smaller coefficient of N^2 than the classical counterpart. Therefore, as N increases, the computational cost of DW_2000Q_6 can be expected to be lower than that of the classical simulated annealing for a certain time. Unfortunately, since the number of qubits in the D-Wave quantum annealer is finite, the potential power of generating mazes by quantum annealing is limited. However, our insight demonstrates some advantages of quantum annealing against its classical counterpart. In addition, we observed that the hybrid solver's computational cost was constant up to $N = 18$. This indicates that hybrid solvers will be potentially effective if they are developed to deal with many variables in the future.

The cost function in this paper has many potential applications by generalizing it. For example, it can be applied to graph coloring and traffic light optimization. Graph coloring can be applied by allowing adjacent cells to have different colors. Traffic light optimization can address the traffic light optimization problem by looking at the maze generation as traffic flow. Roughly speaking, our cost function can be applied to the problem of determining the next state by looking at adjacent states. One of the directions in the future study is in applications of our cost function in various realms. In addition, as described above, we should emphasize that Q_{update} proposed in this paper also has potential use in various fields related to training and education. Then, the powerful computation of quantum annealing and its variants opens the way to such realms with high-speed computation and various solutions.

CONFLICT OF INTEREST STATEMENT

Author Masayuki Ohzeki is employed by Sigma-i. The remaining authors declare that the research was conducted in the absence of any commercial or financial relationships that could be construed as a potential conflict of interest.

AUTHOR CONTRIBUTIONS

Y. I., T. Y., and K. O. conceived the idea of the study. M. O. developed the statistical analysis plan, guided how to use the quantum annealing to find the optimal solution, and contributed to interpreting the results.

Y. I. , T. Y. , and K. O. drafted the original manuscript. M. O. supervised the conduct of this study. All authors reviewed the manuscript draft and revised it critically on intellectual content. All authors approved the final version of the manuscript to be published.

FUNDING

The authors thank financial support from the MEXT-Quantum Leap Flagship Program Grant No. JPMXS0120352009, as well as Public\Private R&D Investment Strategic Expansion Program (PRISM) and programs for Bridging the gap between R&D and the Ideal society (society 5.0) and Generating Economic and social value (BRIDGE) from Cabinet Office.

ACKNOWLEDGMENTS

The authors thank the fruitful discussion with Reo Shikanai on applications of our approach to another application. This paper is the result of research developed from an exercise class held at Tohoku University in Japan in the past called "Quantum Annealing for You, 2nd party!". We would like to thank one of the supporters, Rumiko Honda, for supporting the operations. The participants were a diverse group, ranging from high school students to university students, graduate students, technical college students, and working adults. As you can see from the authors' affiliations, this is a good example of a leap from the diversity of the participants to the creation of academic and advanced content.

REFERENCES

- [Dataset] (2023a). <https://algoful.com/Archive/Algorithm/MazeBar>(accessed 2023-08-13)
- [Dataset] (2023b). <https://algoful.com/Archive/Algorithm/MazeExtend>(accessed 2023-08-13)
- [Dataset] (2023c). <https://algoful.com/Archive/Algorithm/MazeDig>(accessed 2023-08-13)
- Amin, M. H., Andriyash, E., Rolfe, J., Kulchytskyy, B., and Melko, R. (2018). Quantum Boltzmann Machine. *Physical Review X* 8
- Arai, S., Ohzeki, M., and Tanaka, K. (2021a). Mean field analysis of reverse annealing for code-division multiple-access multiuser detection. *Phys. Rev. Research* 3, 033006. doi:10.1103/PhysRevResearch.3.033006
- Arai, S., Ohzeki, M., and Tanaka, K. (2021b). Teacher-student learning for a binary perceptron with quantum fluctuations. *J. Phys. Soc. Jpn.* 90, 074002. doi:10.7566/JPSJ.90.074002
- Bando, Y. and Nishimori, H. (2021). Simulated quantum annealing as a simulator of nonequilibrium quantum dynamics. *Phys. Rev. A* 104, 022607. doi:10.1103/PhysRevA.104.022607
- Bando, Y., Susa, Y., Oshiyama, H., Shibata, N., Ohzeki, M., Gómez-Ruiz, F. J., et al. (2020). Probing the universality of topological defect formation in a quantum annealer: Kibble-zurek mechanism and beyond. *Phys. Rev. Research* 2, 033369. doi:10.1103/PhysRevResearch.2.033369
- Ding, Y., Chen, X., Lamata, L., Solano, E., and Sanz, M. (2021). Implementation of a hybrid classical-quantum annealing algorithm for logistic network design. *SN Computer Science* 2, 1–9
- Feld, S., Roch, C., Gabor, T., Seidel, C., Neukart, F., Galter, I., et al. (2019). A hybrid solution method for the capacitated vehicle routing problem using a quantum annealer. *Frontiers in ICT* 6, 13

- [Dataset] Goto, T. and Ohzeki, M. (2023). Online calibration scheme for training restricted boltzmann machines with quantum annealing
- Haba, R., Ohzeki, M., and Tanaka, K. (2022). Travel time optimization on multi-agv routing by reverse annealing. *Scientific Reports* 12, 17753. doi:10.1038/s41598-022-22704-0
- [Dataset] Hasegawa, Y., Oshiyama, H., and Ohzeki, M. (2023). Kernel learning by quantum annealer
- [Dataset] Hiram, S. and Ohzeki, M. (2023). Efficient algorithm for binary quadratic problem by column generation and quantum annealing
- Hussain, A., Bui, V.-H., and Kim, H.-M. (2020). Optimal sizing of battery energy storage system in a fast ev charging station considering power outages. *IEEE Transactions on Transportation Electrification* 6, 453–463
- Ide, N., Asayama, T., Ueno, H., and Ohzeki, M. (2020). Maximum Likelihood Channel Decoding with Quantum Annealing Machine. In *2020 International Symposium on Information Theory and Its Applications (ISITA)*. 91–95
- Inoue, D., Okada, A., Matsumori, T., Aihara, K., and Yoshida, H. (2021). Traffic signal optimization on a square lattice with quantum annealing. *Scientific reports* 11, 1–12
- Kadowaki, T. and Nishimori, H. (1998). Quantum annealing in the transverse ising model. *Phys. Rev. E* 58, 5355–5363. doi:10.1103/PhysRevE.58.5355
- Khoshaman, A., Vinci, W., Denis, B., Andriyash, E., Sadeghi, H., and Amin, M. H. (2018). Quantum variational autoencoder. *Quantum Science and Technology* 4, 014001
- King, A. D., Suzuki, S., Raymond, J., Zucca, A., Lanting, T., Altomare, F., et al. (2022). Coherent quantum annealing in a programmable 2,000 qubit ising chain. *Nature Physics* 18, 1324–1328. doi:10.1038/s41567-022-01741-6
- Koshikawa, A. S., Ohzeki, M., Kadowaki, T., and Tanaka, K. (2021). Benchmark test of black-box optimization using d-wave quantum annealer. *J. Phys. Soc. Jpn.* 90, 064001. doi:10.7566/JPSJ.90.064001
- Kumar, V., Bass, G., Tomlin, C., and Dulny, J. (2018). Quantum annealing for combinatorial clustering. *Quantum Information Processing* 17, 39. doi:http://doi.org/10.1007/s11128-017-1809-2
- Maruyama, N., Ohzeki, M., and Tanaka, K. (2021). Graph minor embedding of degenerate systems in quantum annealing
- Neukart, F., Compostella, G., Seidel, C., Von Dollen, D., Yarkoni, S., and Parney, B. (2017). Traffic flow optimization using a quantum annealer. *Front. ICT* 4, 29
- Neven, H., Denchev, V. S., Rose, G., and Mcready, W. G. (2012). Qboost: Large scale classifier training with adiabatic quantum optimization. In *Asian Conference on Machine Learning (PMLR)*, 333–348
- Nishimura, N., Tanahashi, K., Suganuma, K., Miyama, M. J., and Ohzeki, M. (2019). Item listing optimization for e-commerce websites based on diversity. *Front. Comput. Sci.* 1, 2
- Orús, R., Mugel, S., and Lizaso, E. (2019). Forecasting financial crashes with quantum computing. *Physical Review A* 99, 060301
- Oshiyama, H. and Ohzeki, M. (2022). Benchmark of quantum-inspired heuristic solvers for quadratic unconstrained binary optimization. *Sci. Rep.* 12, 2146. doi:10.1038/s41598-022-06070-5
- O'Malley, D., Vesselinov, V. V., Alexandrov, B. S., and Alexandrov, L. B. (2018). Nonnegative/binary matrix factorization with a d-wave quantum annealer. *PloS one* 13, e0206653
- Rosenberg, G., Haghnegahdar, P., Goddard, P., Carr, P., Wu, K., and De Prado, M. L. (2016). Solving the optimal trading trajectory problem using a quantum annealer. *IEEE J. Sel. Top. Signal Process.* 10, 1053–1060

- Sato, T., Ohzeki, M., and Tanaka, K. (2021). Assessment of image generation by quantum annealer. *Sci. Rep.* 11, 13523. doi:10.1038/s41598-021-92295-9
- [Dataset] Takabayashi, T. and Ohzeki, M. (2023). Hybrid algorithm of linear programming relaxation and quantum annealing
- Tanaka, T., Sako, M., Chiba, M., Lee, C., Cha, H., and Ohzeki, M. (2023). Virtual screening of chemical space based on quantum annealing. *Journal of the Physical Society of Japan* 92, 023001. doi:10.7566/JPSJ.92.023001
- Urushibata, M., Ohzeki, M., and Tanaka, K. (2022). Comparing the effects of boltzmann machines as associative memory in generative adversarial networks between classical and quantum samplings. *Journal of the Physical Society of Japan* 91, 074008. doi:10.7566/JPSJ.91.074008
- Venturelli, D. and Kondratyev, A. (2019). Reverse quantum annealing approach to portfolio optimization problems. *Quantum Machine Intelligence* 1, 17–30
- [Dataset] Venturelli, D., Marchand, D. J. J., and Rojo, G. (2016). Quantum annealing implementation of job-shop scheduling
- Yamamoto, M., Ohzeki, M., and Tanaka, K. (2020). Fair sampling by simulated annealing on quantum annealer. *J. Phys. Soc. Jpn.* 89, 025002. doi:10.7566/JPSJ.89.025002
- Yonaga, K., Miyama, M., Ohzeki, M., Hirano, K., Kobayashi, H., and Kurokawa, T. (2022). Quantum optimization with lagrangian decomposition for multiple-process scheduling in steel manufacturing. *ISIJ International* 62, 1874–1880. doi:10.2355/isijinternational.ISIJINT-2022-019